Chapter 11

# Reliability Prediction of Smart Maximum Power Point Converter for PV Applications

Giovanna Adinolfi and Giorgio Graditi

Additional information is available at the end of the chapter

http://dx.doi.org/10.5772/intechopen.72130

**Abstract**

The photovoltaic generation distribution supports new energetic scenario development (Net Zero Energy Cluster and DC microgrids). In this context, smart maximum power point (SMPPT) converter represents innovative systems that are able to monitor operating conditions, communicate energetic production data and signal a fault condition. The Smart Maximum Power Point role becomes crucial, and critical aspects such as efficiency and reliability have to be taken into account from the beginning of the design. In this chapter, the idea is to review different reliability prediction models for electronic components focusing on the military ones with the analysis of a case study related to a Smart Maximum Power Point converter in photovoltaic applications.

**Keywords:** MIL-HDBK-217F photovoltaic, reliability, RIAC 217 Plus

## 1. Introduction

Nowadays, photovoltaic (PV) systems are wide and capillary distributed. With the introduction of digital technologies, a new role emerges for these systems. In new scenarios (microgrids [1] and Net Zero Energy Buildings), PV systems become energetic and information "nodes" of the grid. In this context, the efficiency of PV technologies can be improved by the introduction of a smart maximum power point (SMPPT) converter that is able to maximize each photovoltaic generator power by tracking its Maximum Power Point by real-time impedance matching. These converters are characterized by the presence of a digital microcontroller that is able to "manage" the photovoltaic power but also to assure the execution of ancillary services such as monitoring, diagnostics, communication and so on. Crucial aspects are efficiency and reliability; these issues have to be considered since design starting phase. Many prediction models can be used to estimate reliability indices for Smart Maximum Power Point

converters. In this manuscript, the attention is focused on the Military Handbook 217F and its successor RIAC 217 Plus. The case study of a SMPPT Synchronous converter is analyzed.

## 2. SMPPT converter for PV applications

SMPPT converters are DC-DC converters equipped by a suitable control stage. In literature, numerous topological solutions of DC-DC converters [2] have been proposed for PV applications, each of them presenting vantages and critical aspects. Choosing a topology rather than another should be done taking into account the different system parameters in order to determine the optimal solution in terms of cost-benefit analysis.

Topological solution suitable for SMPPT converters can be characterized by synchronous (SR), diode rectification (DR) or interleaved (IL) solutions. In detail, traditional step-up or step-down circuits can be realized with MOSFET for both switching devices, so constituting the SR boost or SR buck. PV application of the most used topology is the boost one reported in the SR, DR and Il versions in **Figure 1**.

IL topology is characterized by a cellular architecture, in which many converters, called cells, are paralleled to create a unique converter. The cells share the same input and output voltages, but each one processes only a fraction of the total system power. One of the primary benefits of a cellular conversion approach is the large degree of input and output ripple cancelation, which can be achieved among cells, leading to reduced ripple in the aggregate input and output waveforms. The active method of interleaving permits to obtain more advantages. In the interleaving method, the cells are operated at the same switching frequency with their switching waveforms displaced

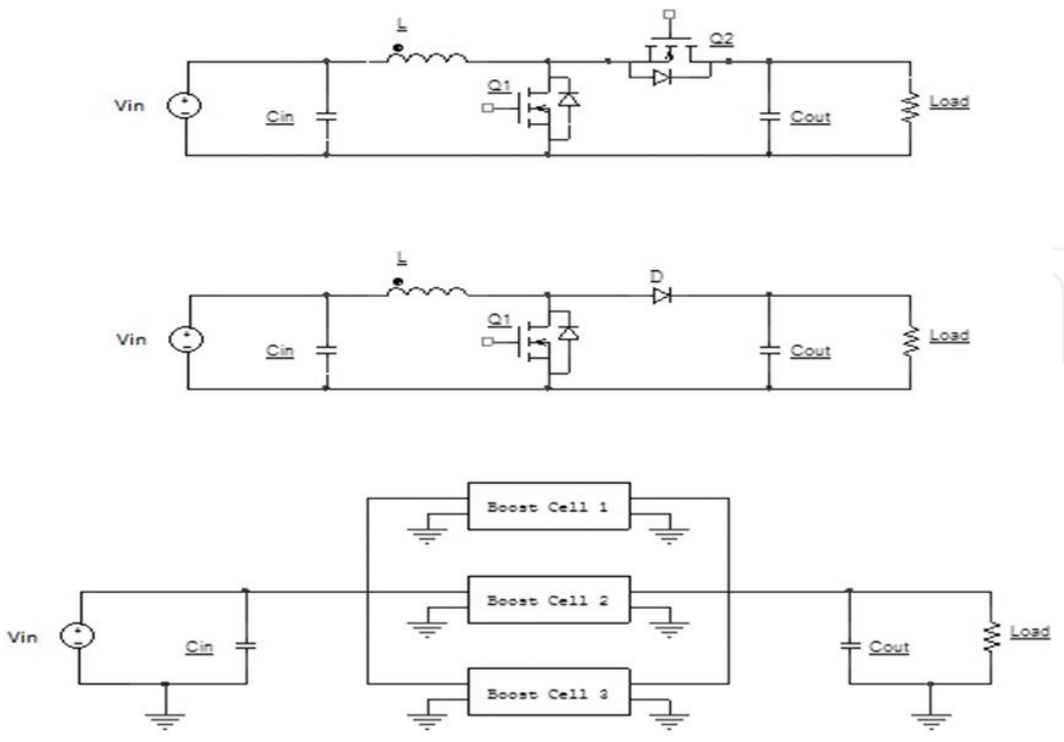


**Figure 1.** SMPPT boost topologies: (a) SR; (b) DR; (c) IL.

in phase over a switching period. The benefits of this technique are due to harmonic cancelation among the cells and include low ripple amplitude and high ripple frequency in the aggregate input and output waveforms. For a broad class of topologies, interleaved operation of N cells yields an N-fold increase in fundamental current ripple frequency, and a reduction in peak ripple magnitude by a factor of N or more compared to synchronous operation. To be effective in cellular converter architecture, however, an interleaving scheme must be able to accommodate a varying number of cells and maintain operation after some cells have failed.

SMPPT converters work in continuous changing conditions as it is evident exploiting historical climatic data series (temperature, irradiance, wind speed) monitored by weather stations [3] and appropriately acquired (**Figure 2**). Since it is difficult to identify the worst operating condition considering both the ambient temperature and the irradiance, the annual frequency of different meteoclimatic conditions can be analyzed in order to identify the most frequent ones.

Both temperature and irradiance effects have to be taken into account to the aim of accurate SMPPT reliability and efficiency estimations. It is possible to identify a joined parameter, the backside temperature $T_{backPV}$, able to represent both temperature and irradiance conditions.

The $T_{backPV}$ formula is reported in Eq. (1).

$$T_{backPV} = T_{PV} + \frac{S}{S_0}\Delta T \tag{1}$$

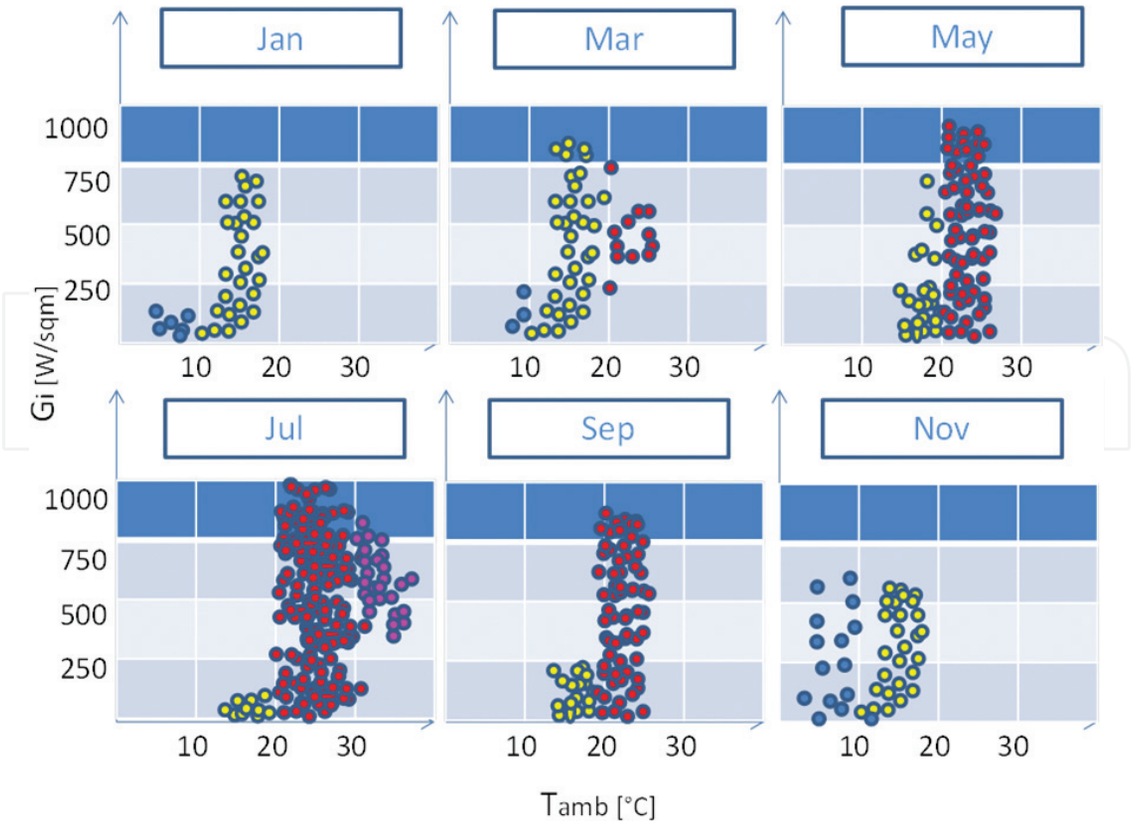


**Figure 2.** Annual distribution of temperature and irradiance.

where

-S is the irradiance at the specific operating condition;

-$S_0$ is 1000 W/m$^2$;

-$T_{PV}$ is the PV generator temperature calculable by means of Eq. (2).

$$T_{PV} = \left(\left(\frac{S}{S_0}\right) * \left(T_1 e^{bw} + T_2\right) + T_a\right) + \frac{S}{S_0}\Delta T \tag{2}$$

where

-$T_a$ is the ambient temperature;

-$T_1$, $T_2$ are empirical coefficients determining upper and lower temperature limits at low wind speeds, in °C;

-b is empirical coefficient determining the rate that module temperature drops as wind speed increases.

## 3. Reliability assessment

The maintenance of correct functioning mode in the time represents an important task for SMPPT converters [4]. This issue involves the concept of reliability evaluation that can be carried out by different reliability prediction model. In detail, the internationally approved definition for the reliability R(t) consists in the probability that an item will perform a required function without failure under stated conditions for a stated period of time. This definition is reported in Eq. (3).

$$R(t) = Pr\{T > t\} \tag{3}$$

where

-t is the mission time;

-T is the unit lifetime.

The reliability value R is a number in the range (0, 1), and its graph is shown in **Figure 3**.

This graph denotes a maximum probability of a system proper functioning at the beginning. This probability decreases with time, and in case of long mission time, the proper functioning probability of a system/device is low.

The reliability of a system can be evaluated by two different types of analysis: the part count analysis (PCA) and the part stress analysis (PSA).

PCA is used in the initial design phase when components and their parameters have not yet been decided. Only the knowledge of the type of components, their level of quality and the environment, in which the system will be used, are necessary.

http://dx.doi.org/10.5772/intechopen.72130

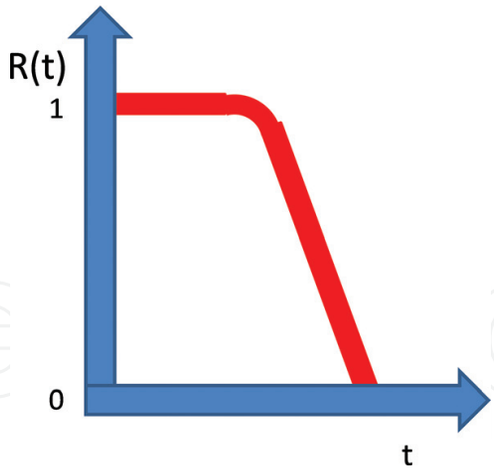


**Figure 3.** Reliability function R(t) graph.

PSA is used in an advanced design phase when the list of system components is known. The failure rate is calculated by considering effects related to the temperature and the electrical stresses to which the devices are subjected.

Various mathematical reliability models [5] are available according to the class of considered components (electronic, electrical, electromechanical devices).

Scientific studies on the reliability of electronic devices have shown that the exponential model represents the suitable one for describing the behavior of these components, as reported in Eq. (4).

$$R(t) = e^{-\lambda t} \tag{4}$$

where

-$\lambda$ is the failure rate;

-t is the mission time.

The exponential distribution is memoryless, and in fact the following expression demonstrates that the probability to have a device lifetime longer than $(t + t_1)$ depends only on $t_1$ and it does not depend on t.

$$Pr\{T > t + t_1 \setminus T > t\} = \frac{Pr\{T > t + t_1\}}{Pr\{T > t\}} = \frac{R(t + t_1)}{R(t)} = \frac{e^{-\lambda(t+t_1)}}{e^{-\lambda t}} = e^{-\lambda t_1} \tag{5}$$

In the case of electronic components, this property means that they only break for accidental causes but not for wear.

### 3.1. Reliability prediction model

As said earlier, many reliability prediction models are available.

The most used ones are:

- MIL-HDBK-217: this reliability model [6], published by the United States Navy in 1965, was the only reliability prediction method available at the time; therefore, the reliability communities adopted this tool for their own use. It is probably the most internationally recognized empirical prediction method. As a result, MIL-HDBK-217 became and is still one of the most widely known and used reliability prediction methods. It includes models for a broad range of part types and supports the five most commonly used environments in the telecom industry (Ground Fixed Controlled, Ground Fixed Uncontrolled, Ground Mobile, Airborne Commercial, and Space) plus additional alternatives useful in the military environment. It is based on pessimistic failure rate assumptions. It does not consider other factors that can contribute to failure rate such as burn-in data, laboratory testing data, field test data, designer experience, wear-out and so on.

- The Telcordia prediction model, Reliability Prediction Procedure for Electronic Equipment SR-332 [7], was developed by AT&T Bell Labs in 1997, and it is focused only on electronic equipment. This model (previously known as Bellcore) modified the MIL-HDBK-217 Prediction Model to better represent the equipment of the telecommunication industry by adding the ability to consider burn-in, field and laboratory test data. Although the Telcordia standard was developed specifically for the telecom field, it is used to model products in a number of other industries. A disadvantage is that the predictions are limited to environment that works with temperature between 30 and 65°C.

- The RIAC Handbook 217 Plus model [8], published in 2006, has been developed by the Reliability Information Analysis Center (RIAC) and pointed out by United States Department of Defense as the successor of the MIL-HDBK-217 and the PRISM methodology. The form of this model is quite different from MIL-HDBK-217 and Telcordia SR-332 because 217 Plus considers a different base failure rate for each generic class of failure mechanism. These process factors are determined by a qualitative assessment of process criteria with weighting factors applied.

- FIDES: the reliability methodology FIDES Guide 2004 [9] has been created by FIDES Group, a consortium of French industrialists from the fields of aeronautics and defense (Airbus France, Eurocopter, GIAT Industries, MBDA and THALES). The FIDES methodology is based on the Prediction Model physics of failures supported by the analysis of test data, so it is different from traditional prediction methods, which are exclusively based on the statistical analysis of historical failure data collected in the field, in-house or from manufacturers.

Many of these models allow to calculate reliability in a specific operating condition. These methods are suitable for a large number of application fields characterized by a worst case or a nominal operating case. In photovoltaic applications, neither a nominal operating condition nor a worst case can be identified. PV systems work, in fact, in constantly changing conditions in terms of irradiance, room temperature, wind speed, humidity and so on. At first analysis, a reliability analysis could be carried out on the worst case, but results would not properly characterize a PV plant since the worst-case scenario is certainly not the condition that

prevalently occurs. The further difficulty is determined by the operation of PV systems which does not, as in other applications, continue. A PV plant does not work 24 h a day for 365 days a year, but a variable number of hours vary depending on different factors, such as sunshine, season and geographic location.

### *3.1.1. Structure connection types*

Another aspect to consider in reliability analysis consists in the structure information and types of connections among the devices of the whole system under investigation. In fact, it is important to consider how the different parts are connected to form the system: In series, in parallel or in series: Parallel combinations. In **Figure 4**, series, parallel and hybrid connections and their respective failure rate formulas are reported.

#### *3.1.1.1. Series connection*

A series structure system (**Figure 4(a)**) functions only when all of its parts are correctly functioning. In this case, the event consisting in the "correct operating mode" S of the system is given by the intersection of the "good functioning" events $A_i$ of the i-parts:

$$S = A_1 \cap A_2 \cap A_3 \ldots\ldots \cap A_N \tag{6}$$

In the assumption that $A_i$ events are stochastically independent, the reliability of the "series" system can be calculated by means of Eq. (7).

$$R_s = Pr\{S\} = \prod_{i=1}^{N} Pr\{A_i\} = \prod_{i=1}^{N} R_i \tag{7}$$

where $R_i$ is the ith part reliability.

The series connection failure rate is calculated as reported in the next formula.

$$\lambda_s(t) = \sum_{i=1}^{N} \lambda_i(t) \tag{8}$$

where $\lambda_i$ is the ith part failure rate.

SMPPT converters characterized by buck and boost topologies are examples of series structures.

#### *3.1.1.2. Parallel connection*

A parallel structure system (**Figure 4(b)**) fails only when every one of its parts fails. The next formula points out that if $\bar{A}_i$ is the "incorrect operation" of the ith part of the system, the event "incorrect operation" of the system is given by the intersection of the different $\bar{A}_i$.

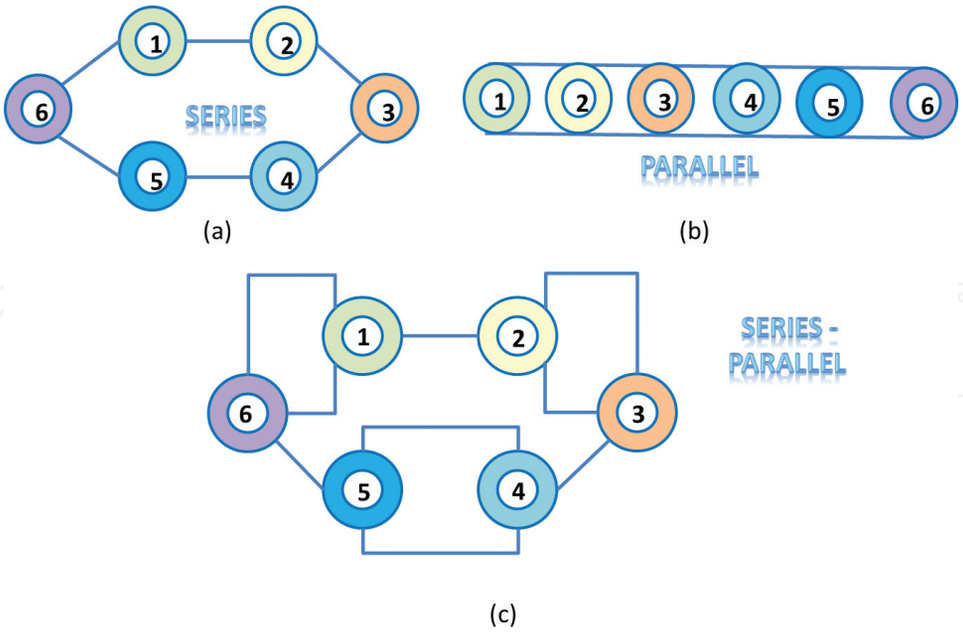


**Figure 4.** Structure connections: (a) series, (b) parallel and (c) series-parallel.

$$\overline{U} = \overline{A_i} \cap \overline{A_2} \cap \overline{A_3} \cap \ldots \cap \overline{A_N} \tag{9}$$

Under the hypothesis of stochastical independence of the event $\bar{A}_i$, the unreliability of a parallel system ($F_p$) can be calculated by the next equation:

$$F_p = Pr\{\overline{S}\} = \prod_{i=1}^{N} Pr\{\overline{A_i}\} = \prod_{i=1}^{N} F_i \tag{10}$$

The reliability of a parallel structure system is reported in Eq. (11).

$$R_s = Pr\{S\} = 1 - \prod_{i=1}^{N} F_i \tag{11}$$

where $F_i$ is the ith part unreliability.

*3.1.1.3. Hybrid connection*

In systems with series-parallel connections (**Figure 4(c)**), the reliability and unreliability functions of the different parts have to be calculated in order to achieve the overall reliability. SMPPT IL converters are examples of hybrid structure, so the designer has to calculate the reliability of its series connections and the unreliability of its parallel connections; finally, the whole system reliability can be evaluated.

*3.1.2. Reliability indices*

Indices used to express devices' reliability performances are as follows:

- the failure rate ($\lambda$) or hazard function that represents the frequency with which a component or a system fails
- the mean time between failure (MTBF) is a measure of how reliable a product is. It is usually given in units of hours. High MTBF values characterize high-reliability products.

The question is:" Which operating condition/s have to be considered to a correct SMPPT reliability evaluation?" The answer is crucial since photovoltaic systems are characterized by operating and nonoperating mode depending on meteorological and climatic conditions and on the day/night alternation. The calculation of reliability indices in a unique working point could not be meaningful. To overcome this drawback, the idea is to propose weighted MTBF formulas obtained by analyzing occurrence of $T_{backPV}$ conditions over an annual time period and identifying the most frequent conditions (**Figure 5**).

In fact, calculating $T_{backPV}$ values and the number of hours they occur, it is possible to obtain $\alpha$ and $\beta$ terms for the weighted MTBF formula:

$$MTBF_{wg} = \alpha_1\, MTBF_{\beta 1} + \alpha_2\, MTBF_{\beta 2} + \alpha_3\, MTBF_{\beta 3} + \alpha_4 MTBF_{\beta 4} + \alpha_5\, MTBF_{\beta 5} \tag{12}$$

In detail, the obtained expression for $MTBF_{wg}$ is reported in Eq. (13).

$$MTBF_{wg} = 0.18\, MTBF_{35\%} + 0.28\, MTBF_{57\%} + 0.19\, MTBF_{71\%} + 0.28 MTBF_{86\%} + 0.07\, MTBF_{100\%} \tag{13}$$

In the followings, the MIL-HDBK-217 and its successor, the RIAC 217 Plus, are analyzed since they represent the most conservative models for reliability prediction.

### 3.2. MIL-HDBK-217F

The Military Handbook 217F can be used for both PCA and PSA analyses.

In case of PCA analysis, the failure rate of the equipment is calculated by the following equation:

$$\lambda_{equip} = \sum_{i=1}^{N} N_i \left(\lambda_g \pi_Q\right)_i \tag{14}$$

where

-$\lambda_g$ is the generic failure rate for the ith component;

-$\pi_Q$ is the quality factor for the ith component;

-$N_i$ is the quantity of the ith component;

-N is the number of different component categories present in the equipment.

Otherwise, in case of PSA analysis, the failure rate of each component is calculated by the following equation:

$$\lambda_p = \lambda_b \ \ \pi_T \pi_A \pi_Q \pi_E \tag{15}$$

where

-$\lambda_p$ is the failure rate, a specific component;

-$\lambda_b$ is the base failure rate of the component in standard condition;

-$\pi_T$ is the temperature factor;

-$\pi_A$ is the application factor;

-$\pi_E$ is the environment factor.

The procedure and the MIL-HDBK-217F formulas to evaluate failure rates of components constituting SMPPT power stage are reported below. In this manuscript, a case study represented by a SMPPT SR boost converter reliability evaluation is presented. The circuit topology is reported in **Figure 1(a)**. This converter is characterized by series connection among electronic devices. As a consequence, the MTBF index, for a specific operating condition, can be calculated as reported in the following formula:

$$MTBF = \frac{1}{\lambda_{Q1+}\lambda_{Q2} + \lambda_L + \lambda_{Cin} + \lambda_{Cout}} \tag{16}$$

*3.2.1. MIL_HDBK-217 F MOSFET failure rate*

In detail, MOSFETs are characterized by failure mechanisms such as defects in the substrate, insulation films or metallization, stress at solder connections due to a mismatch of thermal properties of the different materials and excessive electrical stresses and electrostatic discharges.

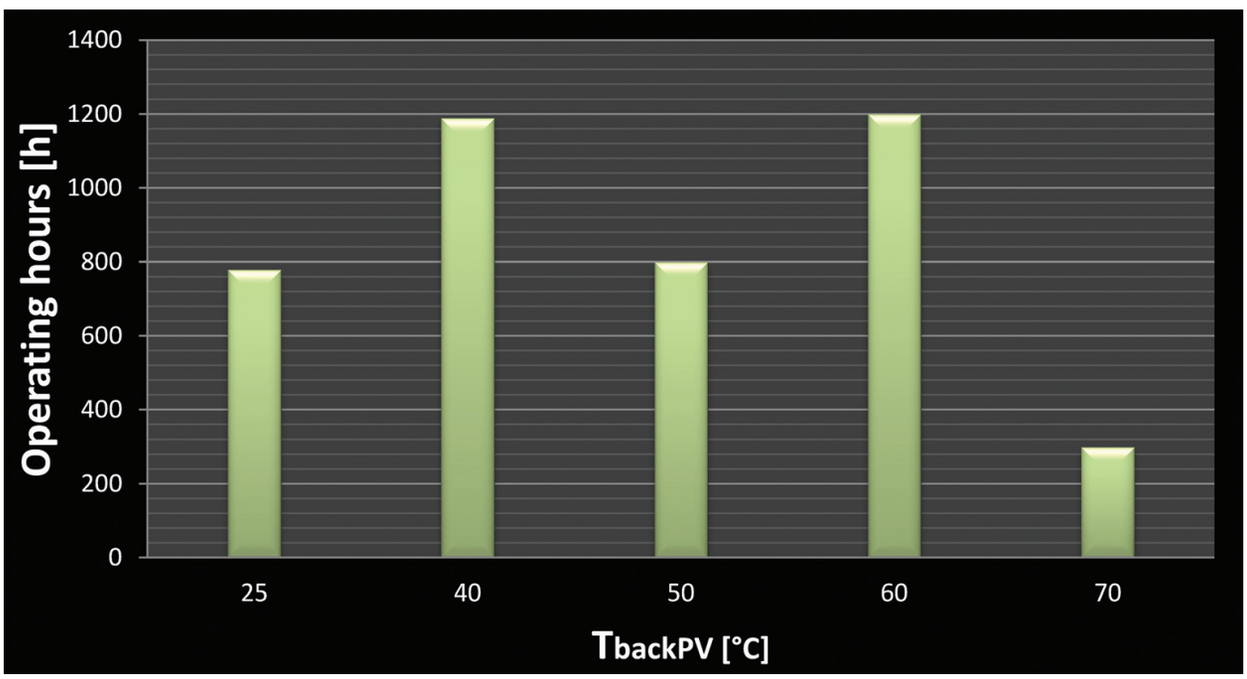


**Figure 5.** $T_{backPV}$ annual distribution.

http://dx.doi.org/10.5772/intechopen.72130

The MOSFET failure rate $\lambda_p$ must be calculated as shown in paragraph 6.4 of MIL_HDBK-217F. The $\lambda_p$ formula is here reported.

$$\lambda_p = \lambda_b \pi_T \pi_A \pi_Q \pi_E \frac{Failures}{10^6\ hours} \tag{17}$$

The base failure rate $\lambda_b$ depends on the transistor typology as indicated in **Table 1**:

SMPPT converters are constituted by MOSFET transistor, so the relative $\lambda_b$ is 0.012.

The application factor $\pi_A$ that depends on the device nominal power is reported in **Table 2**.

In our case study, the MOSFET nominal power is in the range of 80–100 W, so $\pi_A$ is 8.0.

The quality factor $\pi_Q$ values are reported in **Table 3**.

MOSFETs used in SMPPT application are constituted by plastic cases, so the $\pi_Q$ is 8.0.

| **Transistor type** | $\lambda_b$ |
|---|---|
| JFET | 0.0045 |
| MOSFET | 0.012 |

**Table 1.** MIL_HDBK-217 F MOSFET base failure rate.

| **Application** | $\pi_A$ |
|---|---|
| Linear amplification ($P_r < 2W$) | 1.5 |
| Small signal switching | 0.7 |
| Power FETs (non-linear, $P_r \geq 2W$) | |
| $2 \leq P_r < 5\ W$ | 2.0 |
| $5 \leq P_r < 50\ W$ | 4.0 |
| $50 \leq \mathrm{Pr} < 250\ W$ | 8.0 |
| $P_r \geq 250\ W$ | 10 |

**Table 2.** MIL_HDBK-217 F MOSFET application factor values.

| **Quality** | $\pi_Q$ |
|---|---|
| JANTXV | 0.70 |
| JANTX | 1.0 |
| JAN | 2.4 |
| Lower | 5.5 |
| Plastic | 8.0 |

**Table 3.** MIL_HDBK-217 F MOSFET quality factor values.

The value of the environmental factor $\pi_E$ is indicated in **Table 4** for different types of environment.

The MOSFET of the considered converter is installed on the Earth where it is possible to control both the temperature and the humidity, so it is correct to refer to a "Ground Benign" environment and the relative $\pi_E$ -is 1.0.

The temperature factor $\pi_T$ can be obtained by the following equation:

$$\pi_T = e^{\left(-1925\left(\frac{1}{Tj+273}-\frac{1}{298}\right)\right)} \tag{18}$$

where $T_j$ is the MOSFET junction temperature. For example, considering a $T_j$ value of 50°C, the temperature factor is 1.6.

In the considered case study, the SMPPT converter is a synchronous one. As a consequence, the MOSFET failure rate evaluation reported above has to be carried out for both $Q_1$ and $Q_2$.

In detail, as reported before, the Low Side MOSFET $Q_1$ reaches 50°C and the temperature factor is 1.6, while in case of the High Side MOSFET $Q_2$ reaching 40°C, the temperature factor is 1.4.

So, in conclusion, the MOSFET failure rate can be calculated as follows:

$$\lambda_{Q1} = \lambda_b \pi_T \pi_A \pi_Q \pi_E \frac{Failures}{10^6\ hours} = 0.012 * 1.6 * 8 * 8 * 1 = 1.228 \frac{Failures}{10^6\ hours} \tag{19}$$

$$\lambda_{Q2} = \lambda_b \pi_T \pi_A \pi_Q \pi_E \frac{Failures}{10^6\ hours} = 0.012 * 1.4 * 8 * 8 * 1 = 1.075 \frac{Failures}{10^6\ hours} \tag{20}$$

| **Environment** | $\pi_E$ |
|---|---|
| Ground, Benign $G_B$ | 1.0 |
| Ground, Fixed $G_F$ | 6.0 |
| Ground, Mobile $G_M$ | 9.0 |
| Naval, Sheltered $N_S$ | 9.0 |
| Naval, Unsheltered $N_U$ | 19 |
| Airborne, inhabited, Cargo $A_{IC}$ | 13 |
| Airborne, Inhabited, Fighter $A_{IF}$ | 29 |
| Airborne, Uninhabited, Cargo $A_{UC}$ | 20 |
| Airborne, Uninhabited, Fighter $A_{UF}$ | 43 |
| Airborne, Rotary Winged $A_{RW}$ | 24 |
| Space, Flight $S_F$ | 0.5 |
| Missile, Flight $M_F$ | 14 |
| Missile, Launch $M_L$ | 32 |
| Cannon, Launch $C_L$ | 320 |

**Table 4.** MIL_HDBK-217 F MOSFET environment factor values.

*3.2.2. MIL_HDBK-217 F capacitor failure rate*

Formulas and tables to calculate capacitors failure rate are reported in the paragraph 10.1 of the MIL-HDBK-217F.

This evaluation is based on Eq. (21).

$$\lambda_p = \lambda_b \pi_T \pi_C \pi_V \pi_{SR} \pi_Q \pi_E \frac{Failures}{10^6\ hours} \tag{21}$$

where

-$\pi_C$ is the capacitance factor;

-$\pi_V$ is capacitor voltage stress factor;

-$\pi_{SR}$ is the series resistance factor.

The numeric values of these parameters are determined as follows: the basic fault rate $\lambda_b$ depends on the type of capacitors in input and output to the SMPPT converter. Considering an aluminum capacitor working at T Celsius degrees, the $\lambda_b$ is 0.00012 and the $\pi_T$ factor is calculated by the following formula:

$$\pi_T = e^{\left(-\frac{0.35}{8.617*10^{-5}}\left(\frac{1}{T+273}-\frac{1}{298}\right)\right)} \tag{22}$$

The $\pi_C$ factor can be calculated by considering the capacitance value in μF and applying Eq. (23); the $\pi_{SR}$ factor depends on the device equivalent series resistance, and its value is 1.0; the quality factor based on the capacitor plastic case is 10.0.

$$\pi_C = C^{0.23} \tag{23}$$

Finally, also in this case, the environment is "Ground Benign" and the $\pi_V$ factor can be obtained by applying the following formula:

$$\pi_V = \left(\frac{S}{0.6}\right)^5 + 1 \tag{24}$$

So considering the SR input and output capacitor of 120 μF, the relative failure rate is reported as follows:

$$\lambda_{Cin} = \lambda_{Cout} = \lambda_b \pi_T \pi_C \pi_V \pi_{SR} \pi_Q \pi_E = 0.00012 * 1 * 3 * 1 * 1 * 10 * 1 = 0.0036 \frac{Failures}{10^6\ hours} \tag{25}$$

*3.2.3. MIL_HDBK-217F inductor failure rate*

Magnetic devices are the most reliable electronic components. The inductor fault rate $\lambda_p$ is calculated by the following equation reported in Section 11.2 of the Military Handbook.

$$\lambda_p = \lambda_b \cdot \pi_T \cdot \pi_Q \cdot \pi_E \tag{26}$$

In detail, the base failure rate $\lambda_b$ is 0.00003 as in **Table 5**.

The temperature factor formula is reported in Eq. (27).

$$\pi_T = e^{\left(-\frac{0,11}{8,617\cdot10^{-5}}\left(\frac{1}{T_{HS}+273}-\frac{1}{298}\right)\right)} \tag{27}$$

where $T_{HS}$ is the hot-spot temperature.

Similar to previous cases, the $\pi_Q$ and the $\pi_E$ factor can be calculated, and their values are 3.0 and 1.0, respectively.

Considering ad inductor of 47 μH and a $T_{HS}$ of 70°C, the device failure rate is as follows:

$$\lambda_L = \lambda_b \cdot \pi_T \cdot \pi_Q \cdot \pi_E = 0.00003 * 1.767 * 3 * 1 = 1.59 * 10^{-4} \frac{Failures}{10^6 hours} \tag{28}$$

The obtained failure rate confirms the inductor affordable behavior.

After the calculation of the failure rate of the single components, the evaluation of the whole SMPPT converter failure rate is carried out.

$$\begin{aligned} MTBF = \frac{1}{\lambda_{Q1+}\lambda_{Q2} + \lambda_L + \lambda_{Cin} + \lambda_{Cout}} = \frac{1}{1.228 + 1.075 + 1.59 * 10^{-4} + 0.0036 + 0.0036} \\ = 0.433 * 10^6 hours \end{aligned} \tag{29}$$

The reported procedure can be also applied for different SMPPT topologies. Considering the $T_{backPV}$ distribution over an annual period of time, it is possible to calculate the $MTBF_{wg}$ (Eq. (13)) for the analyzed case study.

$$\begin{aligned} MTBF_{wg} = 0.18\, MTBF_{35\%} + 0.28\, MTBF_{57\%} + 0.19\, MTBF_{71\%} + 0.28 MTBF_{86\%} \\ +0.07\, MTBF_{100\%} = 0.2 * 10^6 hours \end{aligned} \tag{30}$$

### 3.3. RIAC 217 Plus

The RIAC Handbook 217 Plus reliability prediction model is the updated version of MIL-HDBK-217F. It guarantees compatibility with its predecessor so keeping unchanged industry practice for systems reliability estimations. It also considers components' operating and nonoperating conditions (operating and nonoperating temperatures, duty cycles, cycling rate and so on). Failure rates are calculated as the product of a base failure rate $\lambda_b$ and some $\pi_i$ factors representing the possible i stresses influencing component reliability.

| **Inductor type** | $\lambda_b$ |
|---|---|
| Fixed | 0.00003 |
| Variable | 0.00005 |

**Table 5.** MIL_HDBK-217 F inductor base failure rate.

In **Table 6**, the 217 Plus failure rate formulas are reported.

where

$\lambda_{OB}$ is base failure rate, Operating;

$\lambda_{EB}$ is base failure rate, Environmental;

$\lambda_{TCB}$ is base failure rate, Temperature Cycling;

$\lambda_{SJB}$ is base failure rate, Solder Joint;

$\lambda_{EOS}$ is failure rate, Electrical OverStress;

$\pi_G$ is reliability growth failure rate factor;

$\pi_{DCO}$ is failure rate factor for Duty Cycle, operating;

$\pi_{TO}$ is failure rate factor for Temperature, operating;

$\pi_S$ is failure rate factor for Stress;

$\pi_{DCN}$ is failure rate factor for Duty Cycle, nonoperating;

$\pi_{TE}$ is failure rate factor for Temperature, environmental;

$\pi_{CR}$ is failure rate factor, Cycling Rate;

$\pi_{DT}$ is failure rate factor, Delta Temperature;

$\pi_{SJDT}$ is failure rate factor, Solder Joint Delta Temperature.

Applying the formulas reported in **Table 6** in a similar manner as the MIL-HDBK-217F model, it is possible to evaluate RIAC 217 Plus reliability performance.

Since the thermal stress is one of the most invalidating factors, the attention is here focused on MTBF variations depending on temperature increase. Referring to the reported failure rate formulas, $\pi_{TE}$ and $\pi_{TO}$ factors for different temperature values are shown in **Figure 6**.

In $\pi_{TE}$ factor graph, the device behavior is similar. In case, instead, of $\pi_{TO}$, the temperature factor considered in operating mode, it is evident the temperature strongly influences the switching and magnetic components. It is worth noting that aspect has to be taken into account for an accurate reliability prediction.

| SMPPT electronic component | Failure rate formulas |
|---|---|
| MOSFET | $\lambda_{MOS} = \pi_G(\lambda_{OB}\pi_{DCO}\pi_{TO}\pi_S + \lambda_{EB}\pi_{DCN}\pi_{TE} + \lambda_{TCB}\pi_{CR}\pi_{DT}) + \lambda_{SJB}\pi_{SJDT} + \lambda_{EOS}$ |
| Diode | $\lambda_{diode} = \pi_G(\lambda_{OB}\pi_{DCO}\pi_{TO}\pi_S + \lambda_{EB}\pi_{DCN}\pi_{TE} + \lambda_{TCB}\pi_{CR}\pi_{DT}) + \lambda_{SJB}\pi_{SJDT} + \lambda_{EOS}$ |
| Capacitor | $\lambda_C = \pi_G\pi_C(\lambda_{OB}\pi_{DCO}\pi_{TO}\pi_S + \lambda_{EB}\pi_{DCN}\pi_{TE} + \lambda_{TCB}\pi_{CR}\pi_{DT}) + \lambda_{SJB}\pi_{SJDT} + \lambda_{EOS}$ |
| Inductor | $\lambda_{Inductor} = \pi_G(\lambda_{OB}\pi_{DCO}\pi_{TO} + \lambda_{EB}\pi_{DCN}\pi_{TE} + \lambda_{TCB}\pi_{CR}\pi_{DT}) + \lambda_{EOS}$ |

**Table 6.** RIAC 217 Plus failure rate formulas.

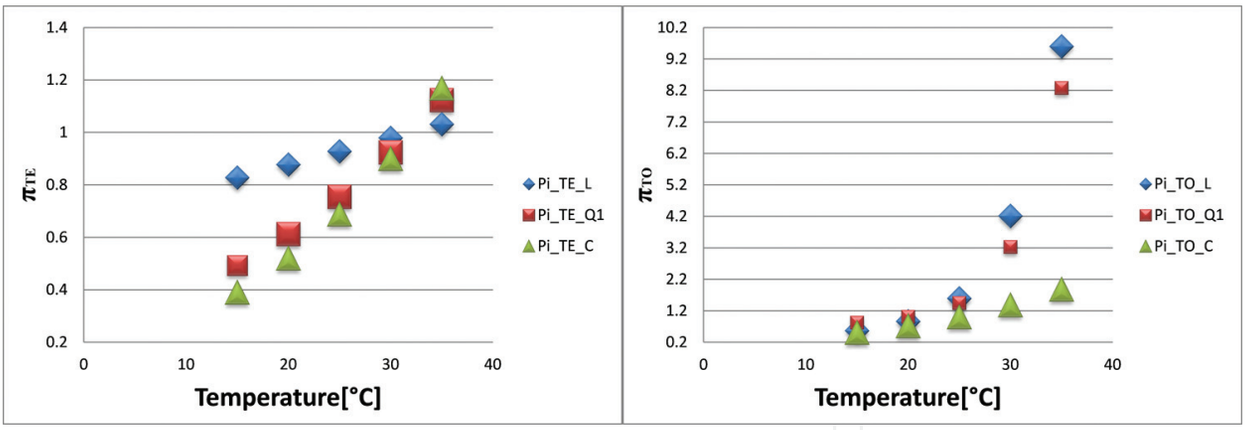


**Figure 6.** RIAC 217+ factors dependence on temperature: (a) $\pi_{TE}$ *vs.* T; (b) $\pi_{TO}$ *vs.* T.

## 4. Reliability comparative analysis among SMPPT topologies

In the last paragraph, the focus is on a comparative analysis among different SMPPT boost converters. In detail, the reliability R(t), considering a period of 25 years (as PV generator one) and an irradiance value of 1000 W/sqm, is calculated for a SR, a DR and an IL boost converter.

Results are reported in Eqs. (31)–(33).

$$R_{SR}(25\ years) = 56\% \tag{31}$$

$$R_{DR}(25\ years) = 68\% \tag{32}$$

$$R_{IL}(25\ years) = 91\% \tag{33}$$

Eqs. (30) and (31) demonstrate that the MOSFET used as High Side switching device in the SR converter appreciably deteriorates the SMPPT reliability performance.

Suitably choosing the IL converter devices, a quasi-redundant or totally redundant structure can be obtained. Such converter is able to assure higher reliability performances than the DR and SR ones as confirmed by Eq. (32).

## 5. Conclusions

In this chapter, reliability prediction models suitable to the evaluation of SMPPT converter performances are considered. The attention is focused on the military models since they provide more conservative predictions with respect to the industrial ones.

A case study about a SMPPT characterized by a SR topology is carried out. In addition, the thermal phenomena influence on the reliability evaluation is showed. Finally, a comparative analysis among SMPPT converters in terms of R (25 years) is obtained, underlining the higher IL boost performances with respect to the SR and DR ones.

## Author details

Giovanna Adinolfi* and Giorgio Graditi

*Address all correspondence to: giovanna.adinolfi@enea.it

ENEA, Italian National Agency for New Technologies, Energy and Sustainable Economic Development, Portici (NA), Italy

## References

[1] Cecati C, Khalid H, Tinari M, Adinolfi G, Graditi G. DC nanogrid for renewable sources with modular DC/DC LLC converter building block. IET power. Electronics. 2017;**9**(5):535-541. DOI: 10.1049/iet-pel.2016.0200

[2] Xiao W, Ozog N, Dunford WG. Topology study of photovoltaic Interface for maximum power point tracking. IEEE Transactions on Industrial Electronics. 2007;**54**(3):1696-1704. DOI: 10.1109/TIE.2007.894732

[3] Ferlito S, Adinolfi G, Graditi G. Comparative analysis of data-driven methods online and offline trained to the forecasting of grid-connected photovoltaic plant production. Applied Energy. 2017;**205**(1). DOI: doi.org/10.1016/j.apenergy.2017.07.124

[4] Calleja H, Chan F, Uribe I. Reliability-oriented assessment of a DC/DC converter for photovoltaic applications. In: Power Electronics Specialists Conference, 2007. PESC 2007. IEEE; 17–21 June 2007; Orlando, USA. IEEE; 2007. DOI: 10.1109/PESC.2007.4342221

[5] Economou M. The merits and limitations of reliability predictions. In: Reliability and Maintainability, 2004 Annual Symposium–RAMS, editors. 26–29 Jan 2004; Los Angeles, CA, USA. USA: IEEE; 2004. DOI: 10.1109/RAMS.2004.1285474

[6] Handbook of Military 217F, 1991, Washington

[7] Telcordia. Reliability prediction procedure for electronic equipment. SR.332, Issue 2, Mar 2016, Sweden

[8] Handbook of 217Plus Reliability Prediction Models. Dec. 2014, Quanterion Solutions, Quanterion Solutions Incorporated, New York

[9] FIDES. Reliability methodology for electronic systems. Guide 2004, Issue A:1-347, Europa

IntechOpen